

Population Pharmacokinetic Modeling of *trans*-Resveratrol and Its Glucuronide and Sulfate Conjugates After Oral and Intravenous Administration in Rats

Helena Colom · Irene Alfaras · Mònica Maijó · M. Emília Juan · Joana M. Planas

Received: 27 July 2010 / Accepted: 8 February 2011 / Published online: 23 March 2011
© Springer Science+Business Media, LLC 2011

ABSTRACT

Purpose To develop a population pharmacokinetic (PK) model which allowed the simultaneous modeling of *trans*-resveratrol and its glucuronide and sulfate conjugates.

Methods Male Sprague–Dawley rats were administered i.v. and p.o. with 2, 10 and 20 mg·kg⁻¹ of *trans*-resveratrol. Blood was collected at different times during 24 h. An integrated PK model was developed using a sequential analysis, with non-linear mixed effect modeling (NONMEM). A prediction-corrected visual predictive check (pcVPC) was used to assess model performance. The model predictive capability was also evaluated with simulations after the i.v. administration of 15 mg·kg⁻¹ that were compared with an external data set.

Results Disposition PK of *trans*-resveratrol and its metabolites was best described by a three-linked two-compartment model. Clearance of *trans*-resveratrol by conversion to its conjugates occurred by a first-order process, whereas both metabolites were eliminated by parallel first-order and Michaelis-Menten kinetics. The pcVPC confirmed the model stability and precision. The final model was successfully applied to the external data set showing its robustness.

Conclusions A robust population PK model has been built for *trans*-resveratrol and its glucuronide and sulfate conjugates that adequately predict plasmatic concentrations.

KEY WORDS glucuronide and sulfate conjugates · NONMEM · polyphenols · population pharmacokinetics · *trans*-resveratrol

ABBREVIATIONS

ABC	ATP-binding cassette
AIC	Akaike information criterion
AUC	area under the curve
BCRP	breast cancer resistance protein
DV	observed concentrations
IAV	inter-animal variability
IPRED	individual model predicted concentrations
MRP	multidrug resistance protein
OFV	objective function value
pcVPC	prediction corrected visual predictive check
PD	pharmacodynamic
PK	pharmacokinetic
PRED	population model predicted concentrations
RSE	relative standard error
UGT	UDP-glucuronosyltransferase

INTRODUCTION

trans-Resveratrol (*trans*-3,4',5-trihydroxystilbene) is found in more than 70 plant species, including grapes, berries and peanuts, where it is biosynthesized in response to different kinds of environmental stress and fungal attack, thus being considered a phytoalexin (1). Furthermore, this polyphenol has been reported to exhibit several beneficial effects on human health, including anti-inflammatory, free-radical scavenging, cardioprotection, immune regulation and anti-tumor activity (1,2). *trans*-Resveratrol also appears to be protective against Alzheimer's and Parkinson's diseases, the

H. Colom (✉)

Departament de Farmàcia i Tecnologia Farmacèutica
Facultat de Farmàcia, Universitat de Barcelona
Av. Joan XXIII s/n
08028 Barcelona, Spain
e-mail: helena.colom@ub.edu

I. Alfaras · M. Maijó · M. E. Juan · J. M. Planas
Departament de Fisiologia, Facultat de Farmàcia
Institut de Recerca en Nutrició i Seguretat Alimentària (INSA-UB)
Universitat de Barcelona
Barcelona, Spain

most common neurodegenerative ailments associated with aging (2). In addition, this polyphenol is well tolerated, and no harmful effects have been reported (3,4).

The pharmacokinetic (PK) information existing for *trans*-resveratrol to date is limited despite that different studies have assessed its oral bioavailability both in animals and humans (4). Previous PK studies included either only one dose (5–7), or the parameters were obtained through non-compartmental analyses (8–10). Moreover, none of them provided an adequate description of the intricate processes that determine the bioavailability of *trans*-resveratrol. After p.o. administration, this compound rapidly enters the intestinal epithelium (11). Once in the enterocyte, it is highly metabolized to glucuro and sulfo-conjugates that are excreted back, in part, to the intestinal lumen through specific proteins from the ATP-binding cassette (ABC) family (11). Therefore, the small intestine comes out as the first bottleneck to the entry of *trans*-resveratrol to the organism. In addition, the metabolism in the liver cannot be underestimated (12,13) before the distribution to tissues where ABC proteins are also present. All these processes influence the distribution and subsequent elimination from the organism (14). As a result of this complex interplay between enzyme activities and efflux transporters, the concentrations of *trans*-resveratrol in plasma have been reported to be low (4).

Consequently, owing to the lack of description of the pharmacokinetics of *trans*-resveratrol and its metabolites, we aim to develop a PK model that can simultaneously describe the pharmacokinetics of both the parent compound and its conjugated metabolites and investigate the linearity of the kinetics after i.v. and p.o. administration of three doses of *trans*-resveratrol in Sprague–Dawley rats. Analyses of the plasmatic data through the population PK approach provides important advantages such as overcoming the limitations of blood sampling in studies using experimental animals and at the same time preserving animal individuality.

MATERIALS AND METHODS

Materials

trans-Resveratrol was purchased from Second Pharma CO., LTD (Shangyu, P.R. China). Dose preparation, rat administration and sample treatments were performed in dim light to avoid photochemical isomerization of *trans*-resveratrol to the *cis* form. Acetonitrile and methanol were purchased from J.T. Baker (Deventer, Netherlands) and acetic acid from Scharlau Chemie S.A. (Barcelona, Spain). All these solvents were HPLC grade. All other reagents were analytical grade and purchased from Sigma-Aldrich (St. Louis, MO, USA). Water used in all experiments was passed through a Milli-Q water purification system (18 m Ω) (Millipore, Milan, Italy).

Animals

The protocol of the present study was reviewed and approved by the Ethic Committee of Animal Experimentation of the University of Barcelona (ref. DMAH-4695). All animal handling followed the European Community guidelines for the care and management of laboratory animals. Male Sprague–Dawley rats (218–432 g) were housed in cages ($n=3$ /cage) under controlled conditions of a 12 h light:dark cycle, with a temperature of $22\pm 3^\circ\text{C}$ and a relative humidity of 40–70%. Water and a standard diet (2014 Teklad Global 14%, Harlan, Spain) were consumed *ad libitum*. No traces of *trans*-resveratrol were detected in the commercial diet as revealed by the analyses performed according to the method described previously (15). All rat manipulations were carried out in the morning to minimize the effects of circadian rhythm.

trans-Resveratrol Administration and Blood Sampling

Overnight fasted rats received a single p.o. or i.v. administration of *trans*-resveratrol at three different doses of $2\text{ mg}\cdot\text{kg}^{-1}$ ($8.8\ \mu\text{mol}\cdot\text{kg}^{-1}$), $10\text{ mg}\cdot\text{kg}^{-1}$ ($43.8\ \mu\text{mol}\cdot\text{kg}^{-1}$) or $20\text{ mg}\cdot\text{kg}^{-1}$ ($87.6\ \mu\text{mol}\cdot\text{kg}^{-1}$). All doses were adjusted according to the rat weight and were freshly prepared immediately before each administration. Given that *trans*-resveratrol is insoluble in water, this compound was solubilized using hydroxypropyl- β -cyclodextrin, a parentally safe excipient. The i.v. administration was performed in a physiological saline solution (0.9% NaCl) of hydroxypropyl- β -cyclodextrin at $1\text{ mL}\cdot\text{kg}^{-1}$ via the tail vein. The p.o. administration was performed in an aqueous solution of hydroxypropyl- β -cyclodextrin (20%, w/v) by gavage at $10\text{ mL}\cdot\text{kg}^{-1}$. Blood was collected from the saphenous vein (16) and placed in tubes containing EDTA-K₂ as anticoagulant (Microvette CB300, Sarstedt, Granollers, Spain). Plasma was immediately obtained by centrifugation at $1500\times g$ (Centrifuge MEGAFUGE 1.0R, Heraeus, Boadilla, Spain) for 15 min at 4°C and was kept at 4°C until analysis, which was performed straight away. Sampling times were 0, 0.016, 0.05, 0.083, 0.16, 0.25, 0.5, 0.75, 1, 1.5, 2, 2.5, 3, 4, 6, 8, 10, 12 and 24 h after administration. A sparse sampling design including 20 rats per dose and route, with 3 to 5 samples per animal, and 5 to 6 values per experimental time were used.

trans-Resveratrol and Its Conjugates Plasmatic Concentrations

Plasma samples were subjected to solid-phase extraction through a reversed-phase C₁₈ Sep-Pak Cartridge (WAT051910, Waters, Mildford, USA), and *trans*-resveratrol and its

glucuronide and sulfate conjugates were analyzed by HPLC as described elsewhere (15). The method was previously validated observing a mean recovery in plasma of 97.4% and linearity ($R^2 > 0.99$) within the range of 0.01–5 $\mu\text{mol}\cdot\text{L}^{-1}$. The intra-day and inter-day precisions were lower than 10%, and the limits of detection and quantification were 1.73 and 5.77 $\text{nmol}\cdot\text{L}^{-1}$, respectively (15).

PK Modeling

Software

A non-compartmental analysis of the plasmatic concentrations of *trans*-resveratrol and its conjugates after i.v. and p.o. administration was carried out with WinNonlin version 3.3 (WinNonlin™ Copyright ©1998–2001, Pharsight Corporation). PK modeling was performed using nonlinear mixed-effects approach implemented in the software NONMEM, version 6.2 (Icon Development Solutions, MD, USA) (17) using the subroutine ADVAN6 (user-defined non-linear model). The first-order conditional estimation method (FOCE) with interaction was used for estimating the model parameters. The Xpose program version 4.2.1 (<http://xpose.sourceforge.net>) implemented into R version 2.11.1 (<http://www.r-project.com>) was used to guide the model-building process (18). Additional graphical and other statistical analysis including evaluation of NONMEM outputs were performed using S-Plus 6.2 for Windows (Insightful, Seattle, WA, USA). The visual predictive check was performed with the Perl speaks-NONMEM (PsN) 3.2.4. Tool-kit (<http://psn.sourceforge.net>) (19).

PK Data Analysis

The areas under the concentrations *vs* time profiles (AUC) from zero to infinity were estimated by non-compartmental analysis using the trapezoidal rule. Then, the individual plasmatic concentrations of *trans*-resveratrol and its glucuronide and sulfate conjugates were analyzed together to allow integrated modeling of parent drug and metabolites using the population modeling approach. Models were fitted to log-transformed concentrations ($\mu\text{mol}\cdot\text{L}^{-1}$). Plasmatic concentrations below the limit of quantification were excluded from the analysis. Inter-animal variability (IAV) was modeled exponentially, assuming a log-normal distribution for the PK parameters. Additive and combined error models on log-transformed data were tested for residual variability modeling of plasmatic concentrations of *trans*-resveratrol and its conjugates. Inclusion of IAV on residual error was also tested in all the cases.

Model selection was based on i) the decrease in the objective function value (OFV; $-2 \times \log$ likelihood); ii)

parameter precision expressed as relative standard error (RSE%) and calculated as the estimate of standard error, obtained as part of the standard NONMEM output, divided by the parameter value; iii) visual inspection of goodness-of-fit plots with Xpose 4.2.1. To statistically distinguish between nested models, the difference in the OFV was used because this difference is approximately χ^2 distributed. A significance level of $p < 0.005$ that corresponded to a difference in OFV of 7.879 for 1 degree of freedom was considered. For non-hierarchical models, the most parsimonious model with the lowest objective function according to the Akaike information criterion (AIC) was chosen (20).

Base Population PK Model

A sequential pharmacokinetic analysis was performed. First, the intravenous concentrations *vs* time data of the parent compound and its conjugates were modeled. Once the best intravenous model was found, the disposition parameters were fixed, and the oral data of the three compounds were added to estimate the absorption parameters (absorption rate constants and bioavailability).

Intravenous Data Modeling. One-, two- and three-compartment linear models were evaluated to characterize the time course of the intravenous plasmatic concentrations of *trans*-resveratrol and its glucuronide and sulfate conjugates. Linear, non-linear or combined (linear and non-linear) elimination kinetics were tested to describe the elimination either of *trans*-resveratrol or of its conjugates. The models were parameterized in terms of distribution clearances (CL_D), apparent volumes of distribution (V), and elimination clearances (CL) for linear elimination processes or maximal elimination rate (V_m) and concentration of the drug at which the elimination is half maximal (K_m), according to the Michaelis-Menten equation.

Oral Data Modeling. According to previous knowledge existing about the kinetics of *trans*-resveratrol and its conjugates (11), pre-systemic metabolism of the parent compound at the enterocyte was tested by simulating simultaneous oral *trans*-resveratrol and equimolar conjugates dosing. A linear process was considered for *trans*-resveratrol absorption; meanwhile, linear, non-linear and combined (linear and non-linear) absorption/conversion processes were tested for the conjugates. Moreover, as it is known that a portion of glucuronide or of sulfate can be effluxed back from the enterocyte to the intestinal lumen (11), it was also tested in the model by allowing for a portion of the parent compound never to be absorbed into the circulation.

Covariate Analysis and Final Model

When the best base intravenous model was found, the covariate body weight was investigated to explain part of the variability between animals. The body weight was evaluated in order to see if part of the IAV observed in the PK parameters (specifically, CL_{Dr} , CL and V_{pg}) could be explained. Once the best base oral model was found, the actual dose was tested in bioavailability to study if linear or non-linear pharmacokinetic behavior took place. In this case, the inclusion of body weight in bioavailability was not considered biologically plausible. Of note, that dose was tested both as a categorical and continuous covariate in the model. Covariates were incorporated in the model when a drop of OFV of more than 7.879, corresponding to a significance level of $p < 0.005$, was observed. The NONMEM code for the final model is included in the Appendix.

Model Validation

A prediction-corrected visual predictive check (pcVPC) was performed to determine whether the final model provides an adequate description of the data (21,22). By using pcVPC, both the observations and model predictions were normalized for the typical model predictions. pcVPCs were constructed with the median, 2.5th and 97.5th percentiles for the observed data, stratifying by compound/administration route. Then, 1000 data sets were simulated from the final model parameter estimates, and the non-parametric 95% confidence intervals for the median, 2.5th and 97.5th percentiles based on the 1000 simulated datasets were calculated and represented together for visual inspection. The extent of the Bayesian shrinkage was also evaluated for each parameter in the final population PK model (23). Large values of shrinkage would be associated with generally poor individual estimates of that parameter.

Model Simulation

Once the final model was proved to be stable through internal validation procedures, its predictive capacity was evaluated by simulating 1000 data sets after the i.v. dose of $15 \text{ mg}\cdot\text{kg}^{-1}$ of the parent compound. The external validation data were obtained using the same experimental conditions (15). The 2.5th, 50th and 97.5th percentiles of the simulated concentrations of *trans*-resveratrol and its conjugates were calculated for each sampling time and plotted together with external observations corresponding to the i.v. dose of $15 \text{ mg}\cdot\text{kg}^{-1}$ for visual inspection.

RESULTS

trans-Resveratrol and Its Conjugates Plasmatic Concentrations

The individual plasma concentrations of *trans*-resveratrol and its conjugates following i.v. and p.o. doses of 2, 10 and $20 \text{ mg}\cdot\text{kg}^{-1}$ are displayed in Figs. 1 and 2. A total of 1039 plasmatic concentrations were obtained for *trans*-resveratrol ($n=449$) and the two conjugates (glucuronide, $n=421$; sulfate, $n=169$) from 120 Sprague–Dawley rats and were used in the final data set. The sampling points adequately defined the overall PK profiles. Plasmatic concentrations were quantified up to 12–24 h post-administration of *trans*-resveratrol with the exception of sulfate conjugate. In this case, plasmatic concentrations were measurable up to around 2 h post-administration after the p.o. doses of 10 and $20 \text{ mg}\cdot\text{kg}^{-1}$ and were not detected after the lowest dose of $2 \text{ mg}\cdot\text{kg}^{-1}$. The total percentages of concentration values below the limit of detection or below the limit of quantification were 2.8%, 4.2% and 27.9% for resveratrol, glucuronide and sulfate, respectively.

PK Modeling

Non-compartmental Analysis

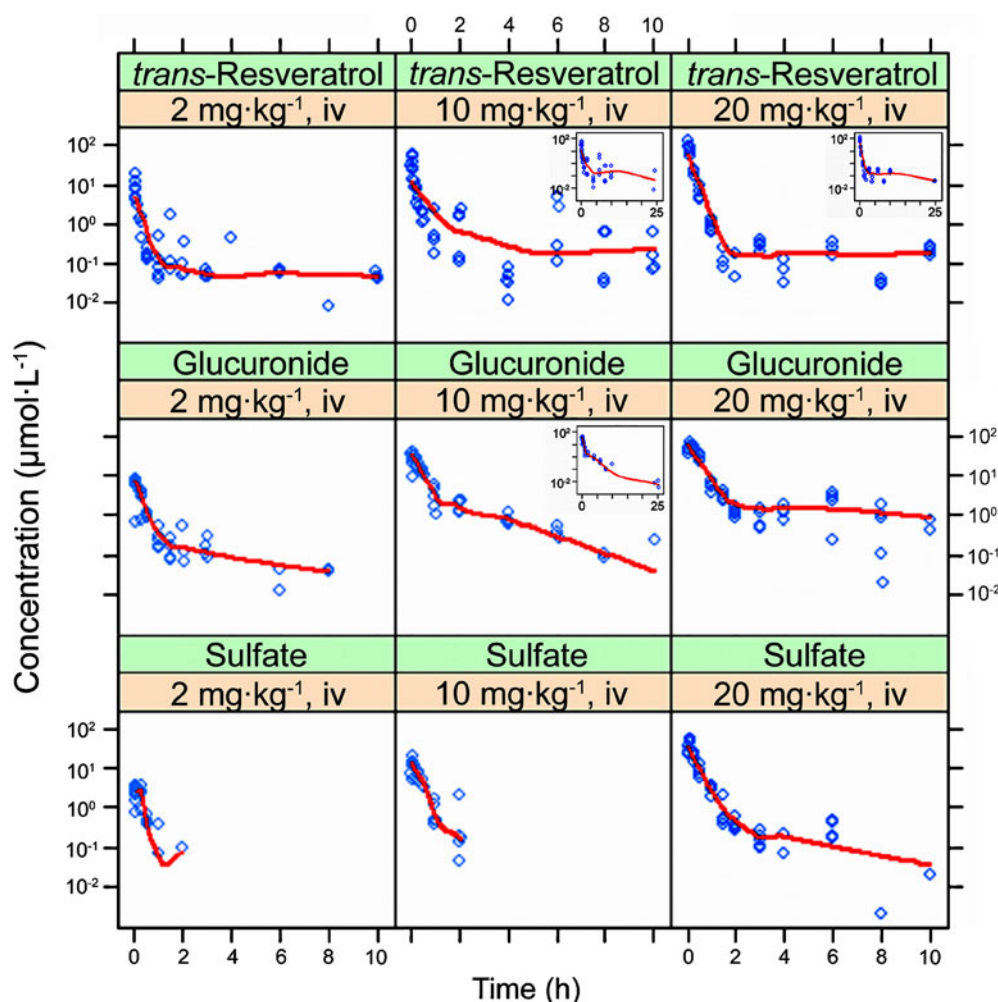
Mean values of AUC estimated from the experimental observations for *trans*-resveratrol and its conjugates after each dose/administration route are indicated in Table I. After i.v. and p.o. administration of 2, 10 and $20 \text{ mg}\cdot\text{kg}^{-1}$, the AUC for *trans*-resveratrol and its conjugates increased with the dose. When AUC was dose normalized (AUC/D), a linear PK behavior was observed for glucuronide and sulfate of *trans*-resveratrol. However, the AUC/D of the parent compound decreased approximately 70% after i.v. administration, while the decrease was 90% in the p.o. administration.

Population PK Model

A schematic of the full model obtained after a sequential population PK analysis is represented in Fig. 3.

Intravenous Data Model. Three-linked two-compartment models were assumed to provide the best intravenous model for both *trans*-resveratrol and its conjugates (glucuronide and sulfate). According to this model, *trans*-resveratrol was administered directly into the central compartment of *trans*-resveratrol (V_{cr}). Once there, all *trans*-resveratrol was assumed to be converted to its glucuronide and sulfate according to first-order elimination

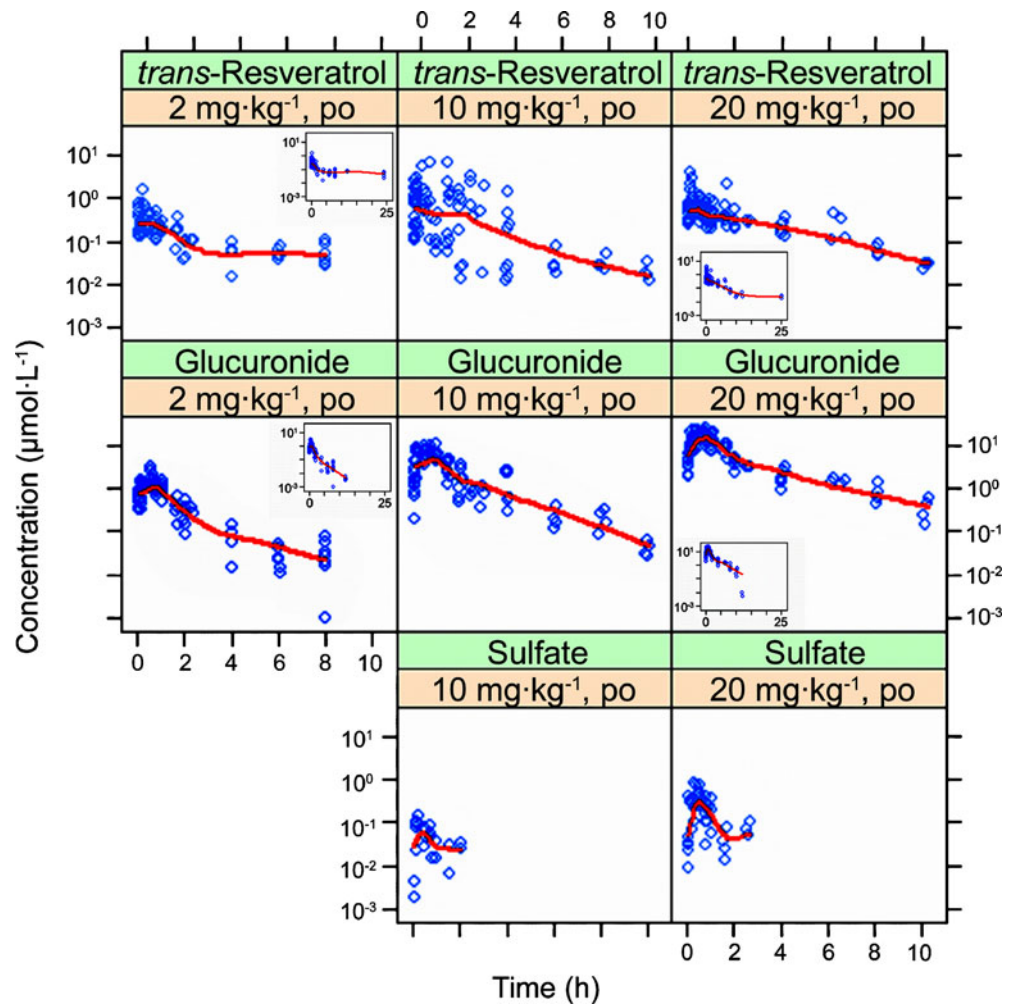
Fig. 1 Plasmatic concentrations vs time profile of *trans*-resveratrol and its glucuronide and sulfate conjugates (circles) after i.v. administration of *trans*-resveratrol at the doses of $2 \text{ mg}\cdot\text{kg}^{-1}$, $10 \text{ mg}\cdot\text{kg}^{-1}$ and $20 \text{ mg}\cdot\text{kg}^{-1}$ in rats. Solid lines represent the trend line of the observed data. The inserts depict the plasmatic concentrations vs time profile from 0 to 25 h.



processes, so two parallel elimination routes were considered. On the other hand, elimination of both metabolites was best described by combined first-order (CL_g and CL_s : clearances associated to the first-order elimination of the glucuronide and sulfate, respectively) and Michaelis-Menten processes (V_{mg} , K_{mg} and V_{ms} , K_{ms} : maximal elimination rates and concentrations of the drug at which the elimination is half maximal for the glucuronide and sulfate, respectively). The inclusion of a parallel Michaelis-Menten elimination process to the linear one, for the glucuronide and sulfate, reduced the AIC values in 17.54 and 3.01 points, respectively. IAV could be included in distributional (CL_{Dr}) and total elimination clearance (CL) of *trans*-resveratrol and peripheral distribution volume of the glucuronide conjugate (V_{pg}). For the other parameters, inclusion of IAV did not improve the fit. Residual error of the three compounds was best described by an additive model on log-transformed data. The clearances associated to the conversion of *trans*-resveratrol to its glucuronide (CL_{fg}) and sulfate (CL_{fs}) were calculated as $CL_{fg} = CL \cdot f_m$, and $CL_{fs} = CL \cdot (1 - f_m)$, where f_m and $1 - f_m$ were the fractions of the parent compound metabolized to the glucuronide

and sulfate conjugates, respectively. Since only the parent compound was administered, this model was *a priori* unidentifiable, and f_m , the distribution volumes and the clearances of formation of both metabolites could not be estimated independently. A simultaneous modeling of *trans*-resveratrol and glucuronide intravenous data, performed in a previous step, provided a V_{cg}/f_m value of 0.0970, under the assumption of $f_m = 1$, i.e. total conversion of the parent compound to the metabolite. Consequently, when the plasmatic sulfate data were incorporated into the modeling process, the V_{cg} value was assumed to be 0.05 for the remaining parameter estimation in order to avoid f_m values > 1 . Then, it was possible to identify f_m , and once f_m was known, $1 - f_m$ could be estimated too, under the assumption that there was no other elimination of *trans*-resveratrol except by formation of glucuronide or sulfate. Therefore, the amount of formed sulfate was known, and the central compartment volume of this metabolite could be identified. By assuming a value for V_{cg} , the clearance values associated to the formation of the metabolites were also identifiable. Of note, the V_{cs} is not necessarily equal to the V_{cg} , but its numerical value is depending on the last. The intravenous

Fig. 2 Plasmatic concentrations vs time profile of *trans*-resveratrol and its glucuronide and sulfate conjugates (circles) after p.o. administration of *trans*-resveratrol at the doses of $2 \text{ mg}\cdot\text{kg}^{-1}$, $10 \text{ mg}\cdot\text{kg}^{-1}$ and $20 \text{ mg}\cdot\text{kg}^{-1}$ in rats. Solid lines represent the trend line of the observed data. The inserts depict the plasmatic concentrations vs time profile from 0 to 25 h.



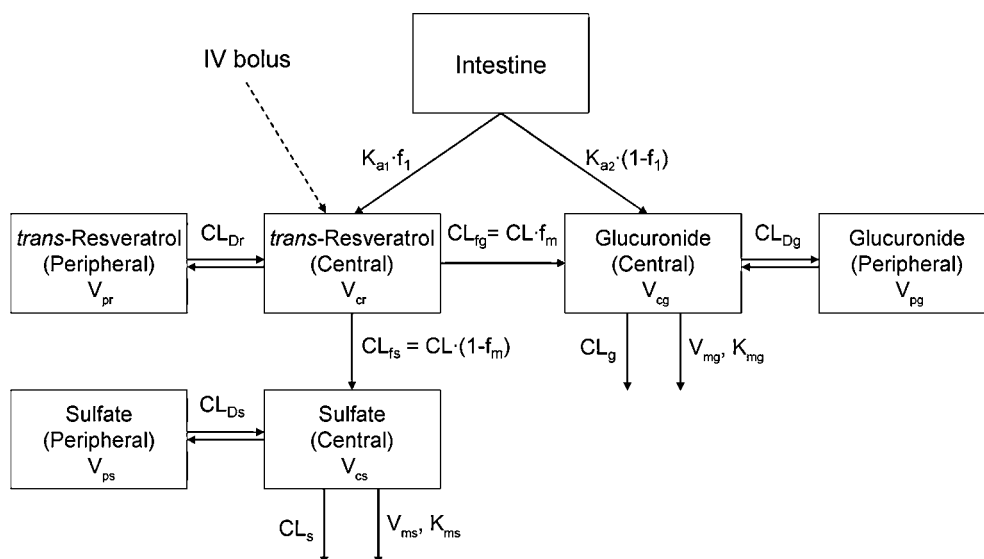
PK base model was assessed both with a full variance-covariance matrix and a diagonal variance-covariance matrix for random-effects. The full matrix did not reduce the OFV, and therefore was not considered further.

Covariate Analysis and Final Intravenous Model. The body weight did not show any significant effect when entered in the intravenous model. The parameter estimates for the final PK intravenous model are given in Table II. The

Table I Mean AUC and AUC Normalized by Actual Doses (AUC/D) Values for *trans*-Resveratrol and Its Conjugates Glucuronide and Sulfate after i.v. and p.o. Doses of 2, 10 and $20 \text{ mg}\cdot\text{kg}^{-1}$

Dose	Intravenous administration		Oral administration	
	AUC ($\mu\text{mol}\cdot\text{L}^{-1}$)·h	AUC/D	AUC ($\mu\text{mol}\cdot\text{L}^{-1}$)·h	AUC/D
<i>trans</i> -Resveratrol				
$2 \text{ mg}\cdot\text{kg}^{-1}$	6.87	2.85	4.04	1.50
$10 \text{ mg}\cdot\text{kg}^{-1}$	19.8	1.53	4.09	0.3
$20 \text{ mg}\cdot\text{kg}^{-1}$	25.8	0.95	3.34	0.12
<i>trans</i> -Resveratrol glucuronide				
$2 \text{ mg}\cdot\text{kg}^{-1}$	5.47	2.27	2.37	0.88
$10 \text{ mg}\cdot\text{kg}^{-1}$	23.2	1.79	14.7	1.09
$20 \text{ mg}\cdot\text{kg}^{-1}$	49.5	1.82	36.3	1.24
<i>trans</i> -Resveratrol sulfate				
$2 \text{ mg}\cdot\text{kg}^{-1}$	1.32	0.55	–	–
$10 \text{ mg}\cdot\text{kg}^{-1}$	6.16	0.48	0.13	0.01
$20 \text{ mg}\cdot\text{kg}^{-1}$	16.48	0.61	0.46	0.02

Fig. 3 Schematic representation of the pharmacokinetic model to simultaneously describe the data of *trans*-resveratrol and its glucuronide and sulfate conjugates after i.v. and p.o. administration. The model consists of three-linked two compartments with first-order absorption process and first-order elimination from the central compartment through the metabolites glucuronide and sulfate. The model also allows the inclusion of the pre-systemic metabolism of *trans*-resveratrol to glucuronide in the intestine.



standard errors of the estimated parameters could not be obtained due to matrix algorithmically singular and algorithmically non-positive semidefinite and covariance step aborted. IAV included in CL, CL_{Dr} and V_{pg} were 19.34%, 90.00% and 61.24%, respectively. Large values of residual variabilities (*trans*-resveratrol: 75.96%; glucuronide: 52.73%; sulfate: 41.35%) were found probably due to analytical contributions and model misspecifications. The mean half-life ($t_{1/2p}$) value of *trans*-resveratrol after i.v. administration calculated from the Bayesian estimations was 0.55 h.

Oral Data Model. Once the disposition parameters were obtained, they were fixed in order to estimate the absorption parameters (absorption rate constants and bioavailability). Therefore, a depot compartment (intestinal compartment) was added to the intravenous model where *trans*-resveratrol was administered. When going into the gastrointestinal tract, *trans*-resveratrol was supposed to be subject to first-pass metabolism and to reach the systemic circulation intact or as its glucuronide. The data did not support the inclusion of first-pass metabolism of *trans*-resveratrol to sulfate, so the model was simplified to absorption/presystemic metabolism of *trans*-resveratrol to its glucuronide and absorption of the formed glucuronide. The inclusion of a fraction of the parent compound never absorbed, and due to metabolism to the conjugates and efflux of them back into intestine, did not improve the fit. The proportions of absorbed intact *trans*-resveratrol and its glucuronide were estimated as f_1 and $(1-f_1)$, respectively. It was assumed that the total absorption of *trans*-resveratrol and its glucuronide was 100%, and the absorption rate for *trans*-resveratrol was rate limiting; hence, the rate of appearance of glucuronide was set to the absorption rate

constant. First-order kinetic processes described the presentation of both *trans*-resveratrol and its glucuronide into the systemic circulation with lower AIC values than Michaelis-Menten kinetics. Different rate constant values for both compounds (*trans*-resveratrol *vs* glucuronide) provided a statistically significant reduction of the OFV in 315.98 points ($p < 0.001$). IAV could only be included in f_1 . Residual error of the three compounds was best described by an additive model on log-transformed data.

Covariate Analysis and Final Oral Model. The covariate analysis showed a dose-dependency behavior in f_1 . The inclusion of dose as a continuous covariate resulted in a higher drop of the OFV than when it was entered as a categorical variable. The inclusion of dose on f_1 reduced the OFV in 81.41 points. The IAV in f_1 was reduced from 96.18% (base model) to 64.80% (final model). According to the final oral model, f_1 decreased significantly with increasing doses from 2 to 20 $\text{mg}\cdot\text{kg}^{-1}$ ($p < 0.001$). Specifically a decrease in f_1 values of 20.62% (from 2 to 10 mg/kg) and 32.12% (from 10 to 20 mg/kg) occurred. The parameter estimates for the oral data model are given in Table II. The RSE of both fixed and random parameters were from 2.70% to 29.29%, which suggests that these parameters were estimated with good precision. As in the intravenous data model, large values of residual variabilities (*trans*-resveratrol: 88.03%; glucuronide: 61.16%; sulfate: 71.62%) were found, probably due to analytical contributions and model misspecifications. Of note, although in the final step of the model development a simultaneous intravenous and oral data modeling was evaluated, the minimization was terminated due to an excess of maximum number of function evaluations and an unreportable number of significant digits.

Table II Population Pharmacokinetic Parameters, Inter-animal and Residual Variability of *trans*-Resveratrol and Its Glucuronide and Sulfate Conjugates after I.V. and P.O. Administration

Parameters	Final model	RSE (%)
Disposition parameters		
<i>trans</i> -Resveratrol	Estimate	RSE (%)
CL (L·h ⁻¹)	1.24	— ^a
V _{cr} (L)	0.249	—
CL _{Dr} (L·h ⁻¹)	0.436	—
V _{pr} (L)	2.80	—
f _m	0.540	—
Glucuronide		
CL _g (L·h ⁻¹)	0.297	—
V _{cg} (L)	0.05	fixed
CL _{Dg} (L·h ⁻¹)	0.127	—
V _{pg} (L)	0.327	—
V _{mg} (μmol·h ⁻¹)	0.0961	—
K _{mg} (μmol·L ⁻¹)	0.00518	—
Sulfate		
CL _s (L·h ⁻¹)	0.737	—
V _{cs} (L)	0.0613	—
CL _{Ds} (L·h ⁻¹)	0.273	—
V _{ps} (L)	0.0770	—
V _{ms} (μmol·h ⁻¹)	0.139	—
K _{ms} (μmol·L ⁻¹)	0.0229	—
Absorption parameters		
K _{a1} (h ⁻¹)	0.442	23.52
f ₁	θ ₁ · (1 - θ ₂ · Dose) ^b	
	θ ₁ = 0.474	12.05
	θ ₂ = 0.0244	2.70
K _{a2} (h ⁻¹)	0.256	7.50
Inter-animal variability ^c		
CL	19.34	—
CL _{Dr}	90.00	—
V _{pg}	61.24	—
f ₁	64.80	29.29
Residual variability ^c		
Intravenous data		
<i>trans</i> -Resveratrol	75.96	—
Glucuronide	52.73	—
Sulfate	41.35	—
Oral data		
<i>trans</i> -Resveratrol	88.03	13.16
Glucuronide	61.16	21.95
Sulfate	71.62	25.34

^a The standard errors of the disposition estimated parameters could not be obtained due to covariance step aborted of the final intravenous data run.

^b Dose values are expressed in μmol.

^c Inter-animal and residual variabilities are expressed as coefficient of variation (CV%).

Intravenous and Oral Data Model Evaluations

Figure 4 illustrates the correlation between observed (DV) and population model-predicted (PRED) and between DV and individual model-predicted (IPRED) concentrations for both intravenous and oral data models. These plots indicated that the models adequately described the concentrations of *trans*-resveratrol and its conjugates. Estimates of η-shrinkage for CL, CL_{Dr}, V_{pg} and f₁ were -2.36, -0.035, 0.15 and -0.28, respectively, while those of ε-shrinkage were 0.37 and 0.20 for intravenous and oral data, respectively. According to these values, shrinkage was present, but it did not affect the correct model selection because it was based on standard model building using the objective function values (23), rather than on empirical bayes estimates (EBE's), IPRED and individual weighted residuals (IWRES). Moreover, the condition number for the oral data model was 8.115, which indicates that the parameter estimates were not severely influenced by ill-conditioning.

Model Validation

The results of the pcVPC stratified by compound (*trans*-resveratrol and its metabolites)/administration route are depicted in Fig. 5. These plots indicated that the model predicts the data adequately in such a way that the 2.5%, 50% and 97.5% percentiles of the observed data overlap the corresponding percentiles of the simulated data.

Model Simulations

According to the results of Fig. 6 the final model showed a satisfactory predictive performance for which there was a close agreement between the observed data found after an i.v. administration of 15 mg·kg⁻¹ of *trans*-resveratrol and model-predicted concentration data for this dose and administration route.

DISCUSSION

The present study performs an integrated PK analysis of *trans*-resveratrol and its glucuronide and sulfate conjugates using a population approach with the non-linear mixed effects modeling. This approach preserves the individuality of plasma concentration profiles and allows the estimation of the typical PK parameters, the corresponding IAV as well as the residual variability. To this end, all the data (from parent compound and conjugates) obtained after the i.v. and p.o. administrations of three doses of *trans*-resveratrol were modeled using a sequential analysis. First, the intravenous data were modeled, and once the disposi-

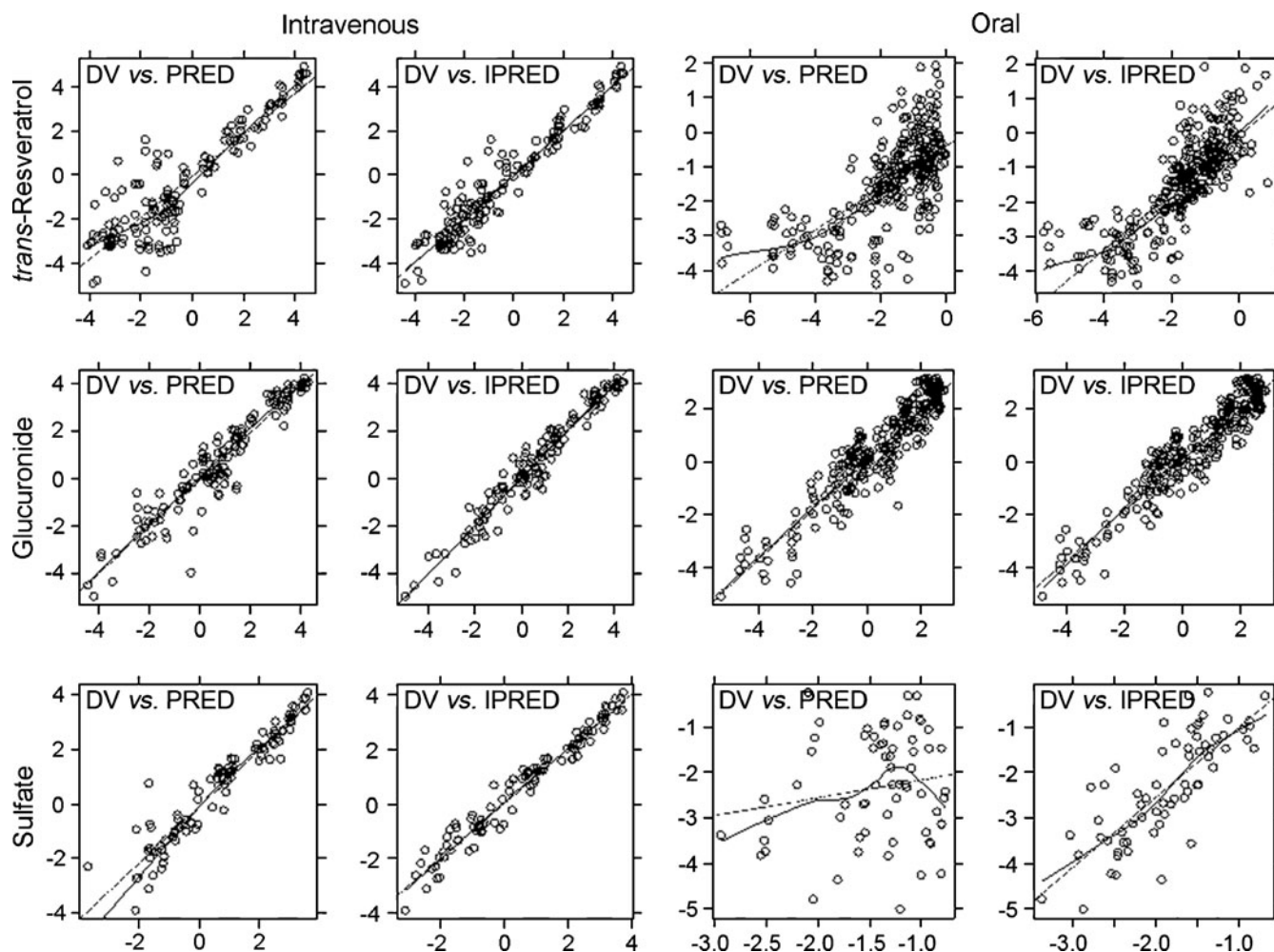


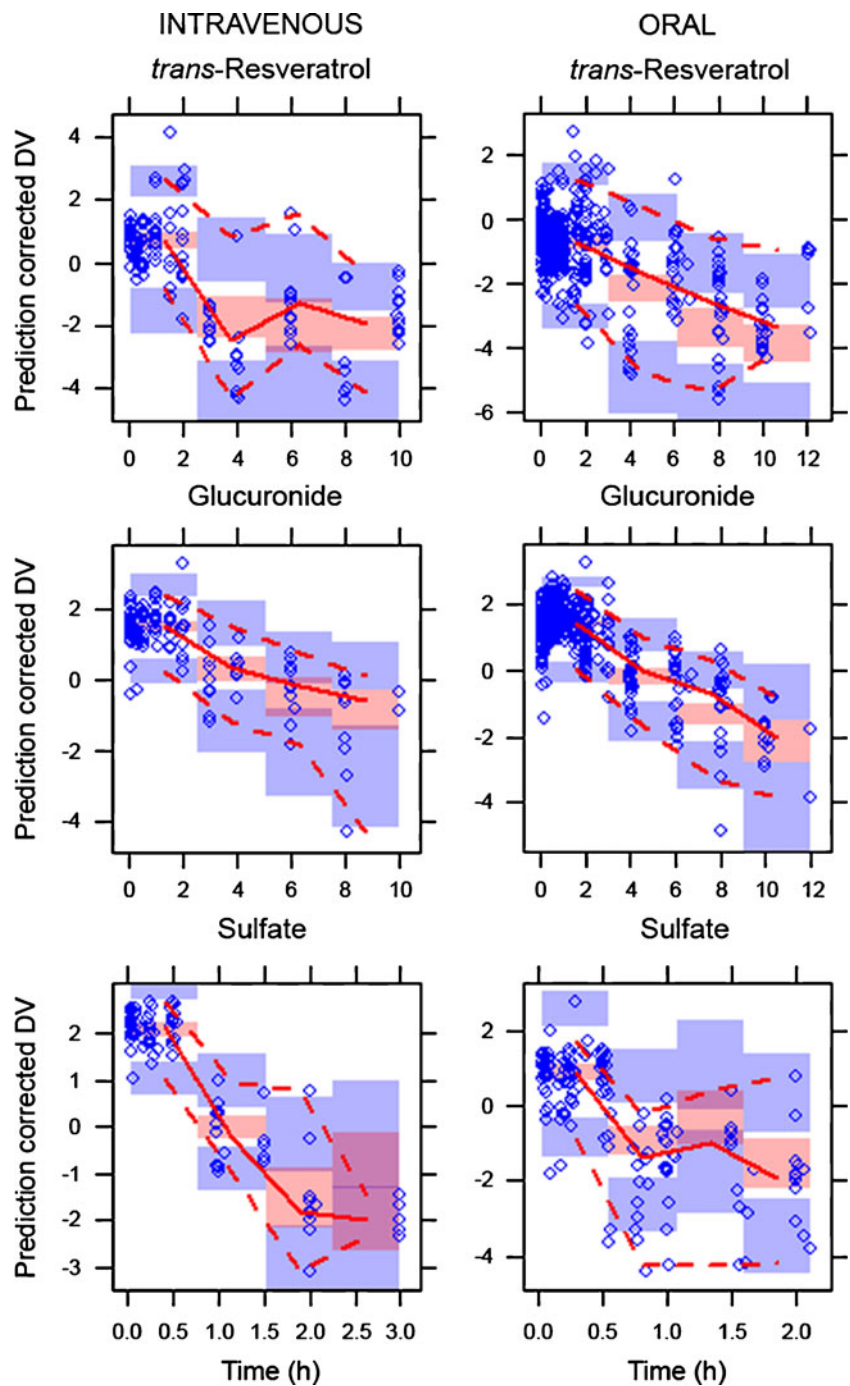
Fig. 4 Goodness-of-fit plots for the final population pharmacokinetic model. The scatter plots show the observed concentrations (DV) vs population model predictions (PRED) and observed concentrations (DV) vs individual model predictions (IPRED). The *dashed lines* represent the identity line; the *solid lines* display the smooth line indicating the general data trend. Concentrations are given in $\mu\text{mol}\cdot\text{L}^{-1}$.

tion parameters were obtained, they were fixed, and the oral data were added in order to estimate the absorption parameters. One-, two- and three-compartment linear models were evaluated to characterize the disposition of *trans*-resveratrol and its conjugates. The best full PK intravenous model was achieved by three-linked two compartments.

Elimination of *trans*-resveratrol by conversion to its glucuronide and sulfate took place by a first-order kinetic process. It is noteworthy that the transformation of the parent compound to its conjugates was not saturable even at the plasmatic concentrations achieved after the highest dose assayed ($20 \text{ mg}\cdot\text{kg}^{-1}$). Meanwhile, clearance of *trans*-resveratrol glucuronide and sulfate was best described by parallel first-order and Michaelis-Menten kinetics. These results are in agreement with existing knowledge about elimination mechanisms of both conjugates (14,24). In

effect, glucuronide and sulfate can suffer either renal or biliar excretion, and in tubular cells and hepatocytes both first-order and Michaelis-Menten kinetics are implicated. The total clearance value of *trans*-resveratrol was slightly higher than $\frac{3}{4}$ times the hepatic blood flow in the rat (0.90 L/h for a body weight of 0.25 kg). According to the f_m value obtained (0.540), approximately the same percentage of both metabolites was formed. Clearances of formation of the glucuronide and sulfate were 0.67 and $0.57 \text{ L}\cdot\text{h}^{-1}$, respectively. Distribution volume of *trans*-resveratrol (total distribution volume = 3.05 L) exceeded the total body water in the rat ($0.15 \text{ L}\cdot\text{kg}^{-1}$ for a body weight of 0.25 kg), suggesting extensive distribution into tissues. A short half-life value was estimated for *trans*-resveratrol (0.55 h) that was in agreement with its clearance and distribution volumes values. By contrast, smaller distribution volumes were found for the metabolites (total distribution

Fig. 5 Prediction-corrected visual predictive check of the pharmacokinetic model for *trans*-resveratrol and its glucuronide and sulfate conjugates after the i.v. and p.o. administrations of 2, 10 and 20 mg·kg⁻¹ of *trans*-resveratrol to rats. The circles represent the observed data. Dashed red lines depict the 2.5th and 97.5th percentiles of the observed concentrations. Solid red lines correspond to the 50th percentiles of the observed concentrations. Shaded blue areas correspond to the 2.5th and 97.5th percentiles and shaded red area to the median calculated from 1000 simulated data sets.



volumes = 0.38 and 0.14 L for the glucuronide and sulfate, respectively).

In the present study, the plasmatic concentrations of *trans*-resveratrol obtained after i.v. and p.o. administration are low and in accordance with previous results obtained by different authors (4–8). The low bioavailability might be explained, at least in part, by the first-pass effect not only in the liver (25–27) but also in the intestine (11,24,28,29). After p.o. administration, *trans*-resveratrol enters to the

enterocyte by simple diffusion (11). Then, this compound undergoes extensive metabolism to its glucuronide and sulfate conjugates (25,26) that are excreted back, in part, to the intestinal lumen through the specific proteins multi-drug resistance protein 2 (MRP2) and breast cancer resistance protein (BCRP) (11). The metabolism in the liver accounted for an extensive glucuronidation and sulfation through UDP-glucuronosyltransferase (UGT) and sulfo-transferase, respectively (4,27). *trans*-Resveratrol and its

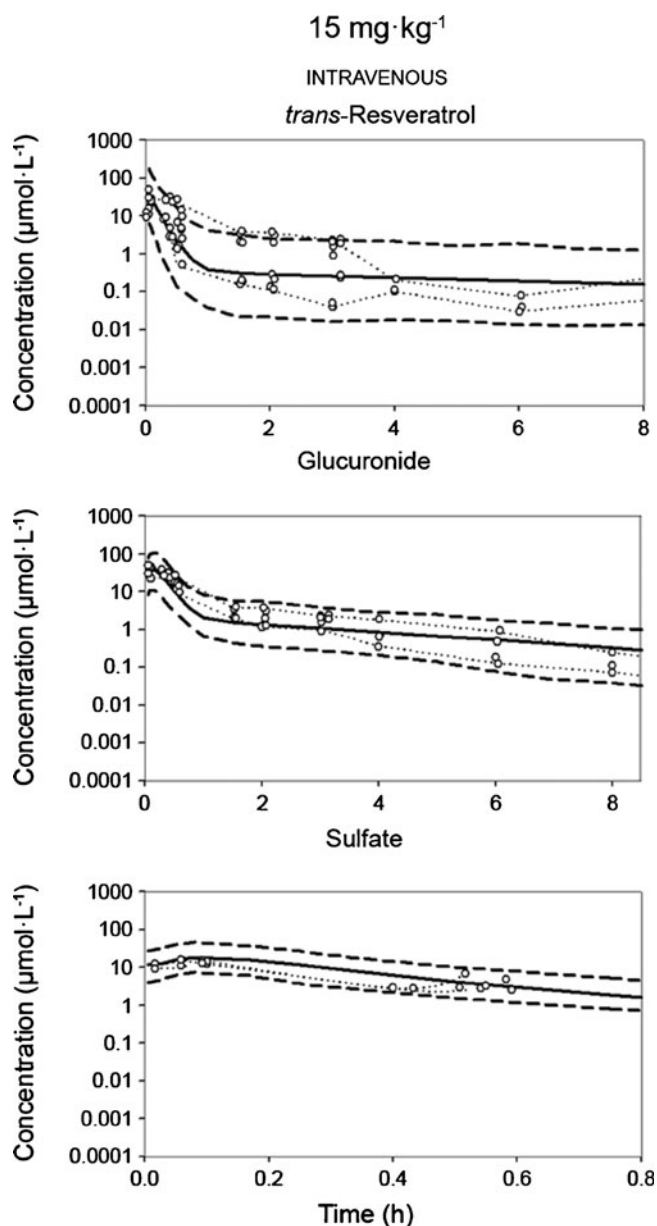


Fig. 6 Model predictive performance of external data. Observed concentrations (circles) of an external data set after an i.v. administration of $15 \text{ mg}\cdot\text{kg}^{-1}$ of *trans*-resveratrol are represented with simulated 50th percentile (solid line) and 2.5th and 97.5th percentiles (dashed lines) and the actual 2.5th and 97.5th percentiles (dotted lines). Simulations ($n=1000$) are based on the final model for an i.v. dose of $15 \text{ mg}\cdot\text{kg}^{-1}$.

conjugates accumulate significantly in this organ (14,15) and are further excreted into the bile, leading to enterohepatic recirculation (6,27). The contribution of the biliar pathways to the elimination of the conjugated metabolites could not be captured by the present model, although a light rebound was observed after 6 h of the i.v. administration, supporting the occurrence of the enterohepatic cycle. Previously, Marier *et al.* (6) have reported that the enterohepatic recirculation using a linked rat model

induced significant increase of plasma concentrations of resveratrol and its glucuronide in bile-recipient rats at 4 to 8 h.

The linearity of the PK after i.v. and p.o. administration of three doses of *trans*-resveratrol was also assessed. The AUC estimated for the parent compound and its conjugated metabolites, by non-compartmental procedures, indicated non-linear PK behavior for *trans*-resveratrol, especially evident after p.o. administration. The linearity of the PK of this polyphenol has scarcely been evaluated previously. Boocock *et al.* (8) performed a pharmacokinetic study after the p.o. administration of 7, 14, 36 and $72 \text{ mg}\cdot\text{kg}^{-1}$ of *trans*-resveratrol in humans. When plotted *vs* dose, the mean AUC and C_{max} values for *trans*-resveratrol increased with dose but in a slightly less than dose-proportional manner, in accordance with our results. The PK behaviors of *trans*-resveratrol and its metabolites in a living animal are somewhat complex. The important role that the intestine plays not only in the absorption process but also in the metabolism of these compounds might explain, at least in part, the differences observed between the oral and intravenous routes (5,14). The lower exposure (AUC) values found after the oral route compared to the intravenous at the three assayed doses could be attributed to the metabolism occurring at the enterocyte as well as the efflux processes from the enterocyte by transporters such as MRP2 or BCRP (11,14).

The uptake of *trans*-resveratrol through the intestine is best fitted with a first-order kinetic. Our plasmatic data of this compound and its glucuronide and sulfate metabolites only allowed the inclusion of the first-pass metabolism in the intestine of *trans*-resveratrol to its glucuronide, but could not take in the conjugation to *trans*-resveratrol sulfate. One of the reasons why *trans*-resveratrol sulfate could not be included in the presystemic metabolism of *trans*-resveratrol might be the low concentrations of this metabolite that reached the bloodstream. These low concentrations could be attributed to a lower sulfation compared to the glucuronidation of *trans*-resveratrol in the rat intestine (28,29). Moreover, the higher affinity and capacity of BCRP for *trans*-resveratrol sulfate compared to the one observed for the glucuronide could account for a higher efficiency in the secretion of the sulfate (24). Andlauer *et al.* (28) appointed that only 0.3% of the absorbed resveratrol reaches the blood as sulfate. Altogether, these processes could explain why the model did not support the inclusion of presystemic metabolism of *trans*-resveratrol to its sulfate conjugate.

In the final model developed, the rate-limiting step is most likely the absorption process of *trans*-resveratrol and its glucuronide rather than the metabolism. The first-order absorption rate constants ($K_{a1}=0.442 \text{ h}^{-1}$, absorption half life = 1.57 h, $K_{a2}=0.256 \text{ h}^{-1}$, absorption/metabolism half life = 2.71 h) confirmed rapid absorption/metabolism kinetics for both compounds. Our results show that when the dose administered increased, a lower fraction of *trans*-resveratrol

remained unchanged ($f_1 = 0.420, 0.207$ and 0.060 for the doses of 2, 10 and $20 \text{ mg}\cdot\text{kg}^{-1}$, respectively, and a body weight of 0.25 kg). By contrast, the relative fraction of glucuronide formed/absorbed from the intestine increased with the dose with values of 0.580, 0.793 and 0.94 for the doses of 2, 10 and $20 \text{ mg}\cdot\text{kg}^{-1}$ and a body weight of 0.25 kg, respectively.

Our work also aimed to develop a PK model for estimation of the time course of *trans*-resveratrol in plasma to be used in future PK-pharmacodynamic (PD) investigation. For this reason, once the model was established and proved to be stable through the internal validation procedures, its predictive capacity was evaluated using an external data set obtained after the i.v. administration of $15 \text{ mg}\cdot\text{kg}^{-1}$. The results showed a close agreement between the observed data and the predicted concentrations for the dose and administration route assayed, supporting the hypothesis of the robustness of the model.

In summary, we built a population PK model to adequately describe plasma data of *trans*-resveratrol and its currently known major metabolites in the rat, including the glucuronide and the sulfate. These data not only increase our knowledge to better understand the PK of this polyphenol but also may be applicable to many other polyphenols which have similar PK properties. In addition the model may also be useful for planning future PK–PD studies to establish the relative contribution of the conjugates to the overall efficacy.

ACKNOWLEDGMENTS

This study was supported by the Ministerio de Ciencia y Tecnología grants AGL2005-05728 and AGL2009-12866 and the Generalitat de Catalunya grants 2005-SGR-00632 and 2009-SGR-00471.

APPENDIX

The NONMEM code used in the final model

Modeling of Intravenous Data

```
$PROBLEM trans-resveratrol and its conjugates plasmatic concentrations
$INPUT ID TIME AMT DV MDV EVID CMT WGT ROUT DOSA;DOSA=ACTUAL DOSE
$DATA data.csv IGNORE=#
IGNORE (ROUT.EQ.2)
$SUBROUTINES ADVAN6 TOL=3
$MODEL
```

```
COMP = (CENTRALRESV,DEFOBS)
COMP = (PERIPHRESV)
COMP = (CENTRALGLUC)
COMP = (PERIPHGLUC)
COMP = (CENTRALSULF)
COMP = (PERIPHSULF)
```

\$PK

```
;DISPOSITION PARAMETERS
```

```
;trans-Resveratrol
```

```
TVCLI = THETA(1)
CL I = TVCLI*EXP(ETA(1)) ;Plasmatic CL of resveratrol
V1 = THETA(2) ;Central compartment V of resveratrol
Q = THETA(3)*EXP(ETA(2)) ;Distributional CL of resveratrol
V2 = THETA(4) ;Peripheral compartment V of resveratrol
```

```
;Glucuronide
```

```
V3 = 0.05 ;Central compartment V of the glucuronide
```

QM1	= THETA(5)	;Distributonal CL of the glucuronide
V4	= THETA(6) *EXP(ETA(3))	;Peripheral compartment V of the glucuronide
;Linear elimination process		
CL2	= THETA(7)	;Plasmatic CL of the glucuronide
;Non-linear elimination process		
VMG	= THETA(8)	;Maximal elimination rate of the glucuronide
KMG	= THETA(9)	;Concentration of the glucuronide at which the elimination is half maximal
FM	= THETA(10)	;Fraction of resveratrol converted to its glucuronide
;Sulfate		
V5	= THETA(11)	;Central compartment V of the sulfate
V6	= THETA(12)	;Peripheral compartment V of the sulfate
QM2	= THETA(13)	;Distributonal CL of the sulfate
;Linear elimination process		
CL3	= THETA(14)	;Plasmatic CL of the sulfate
;Non-linear elimination process		
VMS	= THETA(15)	;Maximal elimination rate of the sulfate
KMS	= THETA(16)	;Concentration of the sulfate at which the elimination is half maximal

;SCALE FACTORS

S1 = V1
S3 = V3
S5 = V5

;RATE CONSTANTS

K12 = Q/V1
K21 = Q/V2
K30 = CL2/V3
K34 = QM1/V3
K43 = QM1/V4
K56 = QM2/V5
K65 = QM2/V6
K50 = CL3/V5

;DIFFERENTIAL EQUATIONS

\$DES

DADT(1)	= -K12*A(1)+K21*A(2)-(CL1/V1)*FM*A(1)-(CL1/V1)*(1-FM)*A(1)
DADT(2)	= K12*A(1)-K21*A(2)
DADT(3)	= (CL1/V1)*FM*A(1)-K30*A(3) + K43*A(4)-K34*A(3)-(VMG*A(3))/(KMG + A(3))
DADT(4)	= K34*A(3)-K43*A(4)
DADT(5)	= (CL1/V1)*(1-FM)*A(1)-K56*A(5) + K65*A(6)-K50*A(5)-(VMS*A(5))/(KMS + A(5))
DADT(6)	= K56*A(5)-K65*A(6)

;RESIDUAL ERROR FOR LOG-TRANSFORMED DATA

\$ERROR

IPRED	= -5
IF(F.GT.0)	IPRED= LOG(F)
IF(CMT.EQ.1)	Y= IPRED + EPS(1)
IF(CMT.EQ.3)	Y= IPRED + EPS(2)


```
IF(CMT.EQ.5)          Y= IPRED + EPS(3)
IWRES                 = (DV-IPRED)
```

```
;INITIAL ESTIMATES
$THETA
$OMEGA
$SIGMA
$ESTIMATION
$COVARIANCE
```

Modeling of Oral Data

```
$PROBLEM trans-resveratrol and its conjugates plasmatic concentrations
$INPUT ID TIME AMT DV MDV EVID CMT WGT ROUT DOSA;DOSA=ACTUAL DOSE
$DATA data.csv IGNORE=#
IGNORE (ROUT.EQ.1)
$SUBROUTINES ADVAN6 TOL=3
$MODEL
```

```
COMP = (DEPOT)
COMP = (CENTRALRESV,DEFOBS)
COMP = (PERIPHRESV)
COMP = (CENTRALGLUC)
COMP = (PERIPHGLUC)
COMP = (CENTRALSULF)
COMP = (PERIPHSULF)
```

```
$PK
```

```
"FIRST
" COMMON/PRCOMG/IDUM1, IDUM2, IMAX, IDUM4, IDUM5
" INTEGER IDUM1, IDUM2, IMAX, IDUM4, IDUM5
" IMAX=70000000
;DISPOSITION PARAMETERS
```

```
;trans-Resveratrol
```

```
TVCLI                 = THETA(1)
CL1                   = TVCLI * EXP(ETA(1))           ;Plasmatic CL of resveratrol
V2                    = THETA(2)                     ;Central compartment V of resveratrol
Q                     = THETA(3) * EXP(ETA(2))       ;Distributional CL of resveratrol
V3                    = THETA(4)                     ;Peripheral compartment V of resveratrol
```

```
;Glucuronide
```

```
V4                    = 0.05                         ;Central compartment V of the glucuronide
QM1                   = THETA(5)                     ;Distributional CL of the glucuronide
V5                    = THETA(6) * EXP(ETA(3))       ;Peripheral compartment V of the glucuronide
FM                    = THETA(7)                     ;Fraction of resveratrol converted to its glucuronide
;Linear elimination process
CL2                   = THETA(8)                     ;Plasmatic CL of the glucuronide
;Non-linear elimination process
VMG                   = THETA(9)                     ;Maximal elimination rate of the glucuronide
KMG                   = THETA(10)                    ;Concentration of the glucuronide at which the elimination is half maximal
```

```
;Sulfate
```

```
V6                    = THETA(11)                    ;Central compartment V of the sulfate
V7                    = THETA(12)                    ;Peripheral compartment V of the sulfate
QM2                   = THETA(13)                    ;Distributional CL of the sulfate
;Linear elimination process
```

CL3 = THETA(14) ;Plasmatic CL of the sulfate
 ;Non-linear elimination process
 VMS = THETA(15) ;Maximal elimination rate of the sulfate
 KMS = THETA(16) ;Concentration of the sulfate at which the elimination is half maximal

;ABSORPTION PARAMETERS

KA1 = THETA(17) ;Absorption rate constant
 KA2 = THETA(18) ;Transformation (from the parent compound to the glucuronide)/Absorption rate constant
 TVFI = THETA(19)*(1-THETA(20))*DOSA
 FI = TVFI*EXP(ETA(4)) ;Bioavailability

;SCALE FACTORS

S2 = V2
 S4 = V4
 S6 = V6

;RATE CONSTANTS

K23 = Q/V2
 K32 = Q/V3
 K40 = CL2/V4
 K45 = QM1/V4
 K54 = QM1/V5
 K67 = QM2/V6
 K76 = QM2/V7
 K60 = CL3/V6

;DIFFERENTIAL EQUATIONS

\$DES

DADT(1) = -KA1*FI*A(1)-KA2*(1-FI)*A(1)
 DADT(2) = KA1*FI*A(1)-K23*A(2)+K32*A(3)-(CL1/V2)*FM*A(2)-(CL1/V2)*(1-FM)*A(2)
 DADT(3) = K23*A(2)-K32*A(3)
 DADT(4) = KA2*(1-FI)*A(1)+(CL1/V2)*FM*A(2)-K40*A(4)+K54*A(5)-K45*A(4)-(VMG*A(4))/(KMG+A(4))
 DADT(5) = K45*A(4)-K54*A(5)
 DADT(6) = (CL1/V2)*(1-FM)*A(2)-K67*A(6)+K76*A(7)-K60*A(6)-(VMS*A(6))/(KMS+A(6))
 DADT(7) = K67*A(6)-K76*A(7)

;RESIDUAL ERROR FOR LOG-TRANSFORMED DATA

\$ERROR

IPRED = -5
 IF(FGT.0) IPRED = LOG(F)
 IF(CMT.EQ.2) Y = IPRED+EPS(1)
 IF(CMT.EQ.4) Y = IPRED+EPS(2)
 IF(CMT.EQ.6) Y = IPRED+EPS(3)
 IWRES = (DV-IPRED)

;INITIAL ESTIMATES

\$THETA
 \$OMEGA
 \$SIGMA
 \$ESTIMATION
 \$COVARIANCE

REFERENCES

1. Pervaiz S, Holme AL. Resveratrol: its biologic targets and functional activity. *Antioxid Redox Signal*. 2009;11(11):2851–97.
2. Brisdelli F, D'Andrea G, Bozzi A. Resveratrol: a natural polyphenol with multiple chemopreventive properties. *Curr Drug Metab*. 2009;10(6):530–46.
3. Juan ME, Vinardell MP, Planas JM. The daily oral administration of high doses of *trans*-resveratrol to rats for 28 days is not harmful. *J Nutr*. 2002;132(2):257–60.
4. Cottart CH, Nivet-Antoine V, Laguillier-Morizot C, Beaudeau JL. Resveratrol bioavailability and toxicity in humans. *Mol Nutr Food Res*. 2010;54(1):7–16.
5. Juan ME, Buenafuente J, Casals I, Planas JM. Plasmatic levels of *trans*-resveratrol in rats. *Food Res Int*. 2002;35(2–3):195–9.
6. Marier JF, Vachon P, Gritsas A, Zhang J, Moreau JP, Ducharme MP. Metabolism and disposition of resveratrol in rats: extent of absorption, glucuronidation, and enterohepatic recirculation evidenced by a linked-rat model. *J Pharmacol Exp Ther*. 2002;302(1):369–73.
7. Sale S, Verschöyle RD, Boocock D, Jones DJ, Wilsner N, Ruparella KC, et al. Pharmacokinetics in mice and growth-inhibitory properties of the putative cancer chemopreventive agent resveratrol and the synthetic analogue *trans* 3, 4, 5, 4'-tetramethoxystilbene. *Br J Cancer*. 2004;90(3):736–44.
8. Boocock DJ, Faust GE, Patel KR, Schinas AM, Brown VA, Ducharme MP, et al. Phase I dose escalation PK study in healthy volunteers of resveratrol, a potential cancer chemopreventive agent. *Cancer Epidemiol Biomark Prev*. 2007;16(6):1246–52.
9. Almeida L, Vaz-da-Silva M, Falcão A, Soares E, Costa R, Loureiro AI, et al. PK and safety profile of *trans*-resveratrol in a rising multiple-dose study in healthy volunteers. *Mol Nutr Food Res*. 2009;53 Suppl 1:S7–15.
10. Nunes T, Almeida L, Rocha JF, Falcão A, Fernandes-Lopes C, Loureiro AI, et al. Pharmacokinetics of *trans*-resveratrol following repeated administration in healthy elderly and young subjects. *J Clin Pharmacol*. 2009;49(12):1477–82.
11. Juan ME, González-Pons E, Planas JM. Multidrug resistance proteins restrain the intestinal absorption of *trans*-resveratrol in rats. *J Nutr*. 2010;140(3):489–95.
12. Hebbar V, Shen G, Hu R, Kim BR, Chen C, Korytko PJ, et al. Toxicogenomics of resveratrol in rat liver. *Life Sci*. 2005;76(20):2299–314.
13. Lançon A, Hanet N, Jannin B, Delmas D, Heydel JM, Lizard G, et al. Resveratrol in human hepatoma HepG2 cells: metabolism and inducibility of detoxifying enzymes. *Drug Metab Dispos*. 2007;35(5):699–703.
14. Alfaras I, Pérez M, Juan ME, Merino G, Prieto JG, Planas JM, et al. Involvement of breast cancer resistance protein (BCRP1/ABC G2) in the bioavailability and tissue distribution of *trans*-resveratrol in knockout mice. *J Agric Food Chem*. 2010;58(7):4523–8.
15. Juan ME, Maijó M, Planas JM. Quantification of *trans*-resveratrol and its metabolites in rat plasma and tissues by HPLC. *J Pharm Biomed Anal*. 2010;51(2):391–8.
16. Hem A, Smith AJ, Solberg P. Saphenous vein puncture for blood sampling of the mouse, rat, hamster, gerbil, guinea pig, ferret and mink. *Lab Anim*. 1998;32(4):364–8.
17. Beal SL, Sheiner LB. NONMEM User's guide. Icon Development Solutions: Ellicott City, MD 1989–2006.
18. Jonsson EN, Karlsson MO. Xpose: an S-PLUS based population pharmacokinetic/pharmacodynamic model building aid for NONMEM. *Comput Meth Programs Biomed*. 1999;58(1):51–64.
19. Lindbom L, Pihlgren P, Jonsson N. PsN-Toolkit: a collection of computer intensive statistical methods for non-linear mixed effect modeling using NONMEM. *Comput Meth Programs Biomed*. 2005;79(3):241–57.
20. Yamaoka T, Nakagawa T, Uno, Application of Akaike's Information Criterion (AIC) in the evaluation of linear pharmacokinetics equations. *J Pharmacokinetic Biopharm*. 1978;6(2):165–75.
21. Karlsson MO, Holford NH. A Tutorial on Visual Predictive Checks. 2008, pp 17 (Abstract 1434). Available at: <http://www.page-meeting.org/?abstract=1434>.
22. Bergstrand M, Hooker AC, Wallin JE, Karlsson MO. Prediction-Corrected Visual Predictive Checks for Diagnosing Nonlinear Mixed-Effects Models. *AAPS J*. 2011. doi:10.1208/s12248-011-9255-z.
23. Savic RM, Karlsson MO. Importance of shrinkage in empirical bayes estimates for diagnostics: problems and solutions. *AAPS J*. 2009;11(3):558–69.
24. van de Wetering K, Burkon A, Feddema W, Bot A, de Jonge H, Somoza V, et al. Intestinal breast cancer resistance protein (BCRP)/Bcrp1 and multidrug resistance protein 3 (MRP3)/Mrp3 are involved in the pharmacokinetics of resveratrol. *Mol Pharmacol*. 2009;75(4):876–85.
25. de Santi C, Pietrabissa A, Mosca F, Pacifici GM. Glucuronidation of resveratrol, a natural product present in grape and wine, in the human liver. *Xenobiotica*. 2000;30(11):1047–54.
26. Sabolovic N, Humbert AC, Radomska-Pandya A, Magdalou J. Resveratrol is efficiently glucuronidated by UDP-glucuronosyltransferases in the human gastrointestinal tract and in Caco-2 cells. *Biopharm Drug Dispos*. 2006;27(4):181–9.
27. Maier-Salamon A, Hagenauer B, Reznicek G, Szekeres T, Thalhammer T, Jäger W. Metabolism and disposition of resveratrol in the isolated perfused rat liver: role of MRP2 in the biliary excretion of glucuronides. *J Pharm Sci*. 2008;97(4):1615–28.
28. Andlauer W, Kolb J, Siebert K, Fürst P. Assessment of resveratrol bioavailability in the perfused small intestine of the rat. *Drugs Exp Clin Res*. 2000;26(2):47–55.
29. Kuhnle G, Spencer JP, Chowrimootoo G, Schroeter H, Debnam ES, Srail SK, et al. Resveratrol is absorbed in the small intestine as resveratrol glucuronide. *Biochem Biophys Res Commun*. 2000;272(1):212–7.